

# The plant ESCRT component FREE1 shuttles to the nucleus to attenuate abscisic acid signalling

Hongbo Li<sup>1,5</sup>, Yingzhu Li<sup>1,5</sup>, Qiong Zhao<sup>2,5</sup>, Tingting Li<sup>1</sup>, Juan Wei<sup>1</sup>, Baiying Li<sup>2</sup>, Wenjin Shen<sup>1</sup>, Chao Yang<sup>1</sup>, Yonglun Zeng<sup>2</sup>, Pedro L. Rodriguez<sup>3</sup>, Yunde Zhao<sup>4</sup>, Liwen Jiang<sup>2\*</sup>, Xiaojing Wang<sup>1\*</sup> and Caiji Gao<sup>1\*</sup>

**The endosomal sorting complex required for transport (ESCRT) machinery has been well documented for its function in endosomal sorting in eukaryotes. Here, we demonstrate an up-to-now unknown and non-endosomal function of the ESCRT component in plants. We show that FYVE DOMAIN PROTEIN REQUIRED FOR ENDOSOMAL SORTING 1 (FREE1), a recently identified plant-specific ESCRT component essential for multivesicular body biogenesis, plays additional functions in the nucleus in transcriptional inhibition of abscisic acid (ABA) signalling. Following ABA treatment, SNF1-related protein kinase 2 (SnRK2) kinases phosphorylate FREE1, a step requisite for ABA-induced FREE1 nuclear import. In the nucleus, FREE1 interacts with the basic leucine zipper transcription factors ABA-RESPONSIVE ELEMENTS BINDING FACTOR4 and ABA-INSENSITIVE5 to reduce their binding to the *cis*-regulatory sequences of downstream genes. Collectively, our study demonstrates the crosstalk between endomembrane trafficking and ABA signalling at the transcriptional level and highlights the moonlighting properties of the plant ESCRT subunit FREE1, which has evolved unique non-endosomal functions in the nucleus besides its roles in membrane trafficking in the cytoplasm.**

The endosomal sorting complex required for transport (ESCRT) machinery is an evolutionarily conserved system, which consists of several multi-subunit subcomplexes designated ESCRT-0, -I, -II and -III as well as accessory proteins. The major and canonical functions of ESCRT are to regulate multivesicular body (MVB) biogenesis and to sort ubiquitinated membrane cargoes into the intraluminal vesicles inside MVBs, which then fuse with the vacuole or lysosome to release the membrane cargoes that reside in intraluminal vesicles into the vacuole lumen for degradation<sup>1,2</sup>. In the past few years, most of the putative paralogues of ESCRT components have been identified in plants, with the exception of the highly variable ESCRT-0 components and the ESCRT-I subunit Mvb12 (refs. <sup>3,4</sup>). In addition, the essential functions of several ESCRT paralogues in MVB biogenesis and MVB-mediated endosomal sorting have been well documented in plants<sup>5–7</sup>. More strikingly, plants seem to evolve unique ESCRT components with limited sequence similarities to the known ESCRT proteins in eukaryotes. For example, studies from our and other groups have identified FYVE DOMAIN PROTEIN REQUIRED FOR ENDOSOMAL SORTING 1 (FREE1 (also known as FYVE1)) as a plant-specific and phosphatidylinositol 3-phosphate (PtdIns3P)-binding protein, which is incorporated into the ESCRT complexes via interaction with other components, including vacuolar protein sorting-associated protein 23 (VPS23), SNF7 and AtBRO1/ALIX, to regulate multiple endosomal steps, such as MVB-mediated ubiquitinated protein sorting, MVB biogenesis and vacuolar transport<sup>8–10</sup>. FREE1 was also demonstrated to interact with SH3P2 and SH3P3, in which SH3P2 has been shown to function as a unique regulator of plant autophagy<sup>9,11</sup>, to modulate autophagosome–vacuole

fusion and autophagic degradation in plants<sup>12</sup>. Moreover, it has also been shown that FREE1 interacts with IRON-REGULATED TRANSPORTER 1 (IRT1) to modulate IRT1-dependent metal transport and metal homeostasis in plants<sup>13</sup>. Because of its essential and multiple functions in several cellular processes, FREE1 loss-of-function mutant plants display seedling lethality.

Owing to their unique ability to regulate MVB-mediated membrane protein degradation, and thereby downregulation of cell-surface receptors, it is not a surprise to see the participation of ESCRT proteins in intracellular signalling events, which are well manifested by recent studies showing the involvement of ESCRT in plant hormone abscisic acid (ABA) signalling. ABA is first perceived by the PYRABACTIN RESISTANCE1 (PYR1)/PYR1-LIKE (PYL)-REGULATORY COMPONENTS OF ABA RECEPTORS (RCAR) receptors<sup>14</sup>. This is followed by interaction with and inactivation of clade A protein phosphatase type 2Cs (PP2Cs), thereby releasing the ABA-activated sucrose non-fermenting 1-related protein kinases (SnRK2s) for further activation of downstream signalling cascade through phosphorylation<sup>15–17</sup>. Recent advances in the field of ABA signalling have shown that a proportion of membrane-associated and ubiquitinated PYR/PYL-RCAR receptors can be captured by the ESCRT-I components FREE1 and VPS23A in regions reminiscent of endosomes, followed by the MVB-mediated sorting into vacuole for degradation<sup>18,19</sup>. The mutant plants with knockdown of *FREE1* or depletion of VPS23A accumulate more ABA receptors, such as PYL4, and show hypersensitivity to ABA treatment<sup>18,19</sup>. The plasma membrane-localized proteins, including the RING E3 ligase RSL1 and the C2-domain ABA-related (CAR) proteins, presumably help to regulate the ubiquitination and membrane association of

<sup>1</sup>Guangdong Provincial Key Laboratory of Biotechnology for Plant Development, School of Life Sciences, South China Normal University (SCNU), Guangzhou, China. <sup>2</sup>School of Life Sciences, Centre for Cell & Developmental Biology and State Key Laboratory of Agrobiotechnology, The Chinese University of Hong Kong, Shatin, Hong Kong, China. <sup>3</sup>Instituto de Biología Molecular y Celular de Plantas, Consejo Superior de Investigaciones Científicas-Universidad Politécnica de Valencia, Valencia, Spain. <sup>4</sup>Section of Cell and Developmental Biology, University of California, San Diego, La Jolla, CA, USA. <sup>5</sup>These authors contributed equally: Hongbo Li, Yingzhu Li, Qiong Zhao. \*e-mail: [ljjiang@cuhk.edu.hk](mailto:ljjiang@cuhk.edu.hk); [wangxj@scnu.edu.cn](mailto:wangxj@scnu.edu.cn); [gaocaiji@m.scnu.edu.cn](mailto:gaocaiji@m.scnu.edu.cn)

PYR/PYL-RCAR receptors during their ESCRT-dependent sorting into the vacuole for degradation<sup>20,21</sup>. Thus, plant ESCRT components can function to attenuate ABA signalling by regulating the turnover of ABA receptors.

Although the general concept that FREE1 plays important roles in plant endosomal sorting is established<sup>8,9,12</sup>, the seedling lethality of FREE1 depletion mutants hinders the study of FREE1 function in established seedling stage. To further elucidate the molecular functions of FREE1 in endosomal sorting and to dissect the functional necessity of FREE1 in plant responses to growth and environmental signals, we recently performed a high-throughput suppressor screen to find *sof* (suppressor of *free1*) mutants that can rescue the *free1* seedling lethal phenotype using inducible FREE1-RNA interference (RNAi) plants, and also tried to generate mutants with a *free1* weak allele with domain deletions or mutations of FREE1 using the clustered regularly interspaced short palindromic repeats (CRISPR)–CRISPR-associated protein 9 (Cas9) system<sup>22</sup>. In a most recent study, we identify the *sof524* mutant, which is due to a loss of function in an *Arabidopsis* Bro1-domain protein termed BRAF and further demonstrate that BRAF regulates MVB biogenesis and membrane protein sorting by modulating the endosomal recruitment of FREE1 (ref. 23).

Here, we extended our previous study and demonstrated an unexpected and non-endosomal function of FREE1 in the nucleus by using a newly established *free1* weak mutant allele with a defect in the nuclear import of FREE1. We found the phosphorylation-dependent nucleocytoplasmic shuttling of FREE1 and discovered an unexpected role of nuclear-localized FREE1 in attenuating ABA signalling by reducing the transcriptional activation activities of ABA-responsive transcription factors, including ABI5 and ABF4. Our results uncover a hitherto unknown function of the plant ESCRT component in transcriptional regulation in the nucleus and highlight the dual-function nature of FREE1 in ABA signalling.

## Results

**The C-terminal coiled-coil domain of FREE1 confers ABA hypersensitivity response as revealed by using a newly created *free1-ctmut* plant.** In this study, we circumvented the lethality of the *free1* loss-of-function mutant and generated a *free1* weak allele termed *free1-ctmut* using the CRISPR–Cas9 system as described previously<sup>24,25</sup>. Sanger sequencing of the *FREE1* genomic DNA sequence from the *free1-ct* mutant revealed an 8-bp deletion within the penultimate exon (Fig. 1a), which results in a premature stop codon in the *FREE1* protein sequence at the 581 amino acid site with an introduction of foreign polypeptides of 26 amino acid residues from 558 to 581 (Fig. 1b). Detection of endogenous FREE1 with a smaller size in the *free1-ctmut* plant by immunoblotting with FREE1 antibody suggested the production of truncated FREE1 protein with a deletion of the carboxy-terminal tail (Fig. 1c). The *free1-ctmut* mutant showed no obvious phenotype under regular growth condition, but displayed enhanced sensitivity to ABA-mediated inhibition of seedling establishment and ABA-induced detached leaf senescence compared to the wild-type (WT) plant (Fig. 1 and Supplementary Fig. 1). The F1 plants of *free1-ctmut* crossed with WT resembled the WT in terms of ABA response, suggesting that the *free1-ctmut* mutation is recessive (Supplementary Fig. 1).

The FREE1 protein has three known domains, including the amino-terminal intrinsically disordered region, the FYVE domain and the C-terminal coiled-coil region, in which the FYVE domain is shown to be responsible for binding to the PtdIns3P lipid<sup>8</sup>. To gain insight into the functions of different domains of the FREE1 protein in conferring ABA hypersensitivity of the *free1-ctmut* plant, four versions of green fluorescent protein (GFP) fusions with FREE1, FREE1-CTmut, FREE1( $\Delta$ FYVE) and FREE1( $\Delta$ CC) were individually introduced into *free1-ctmut* followed by phenotypic analysis in response to ABA. As shown in Fig. 1d–f, full-length

FREE1 fully complemented the ABA-hypersensitive phenotypes of *free1-ctmut*, whereas the C-terminal truncated version, including FREE1-CTmut and FREE1( $\Delta$ CC), failed to complement the *free1-ctmut* phenotype, highlighting the functional importance of the FREE1 C terminus in conferring ABA hypersensitivity of the *free1-ctmut* plant. Intriguingly, FREE1( $\Delta$ FYVE) with truncation of the FYVE domain, which failed to recover the lethality of the *free1* mutant (Supplementary Fig. 2), could largely complement the ABA-hypersensitive phenotype of *free1-ctmut* (Fig. 1). A previous study found that the N-terminal part of FREE1 (amino acid residues 1–395) was responsible for its interaction with the ABA receptors, thereby mediating the MVB-mediated sorting and degradation of ABA receptors in the vacuole<sup>18</sup>. Knockdown of *FREE1* leads to hypersensitivity of the mutant plants to ABA due to the accumulation of ubiquitinated PYLs that failed to be sorted into the intraluminal vesicles inside MVBs<sup>18</sup>. In this newly established *free1-ctmut* plant, the deletion part is located in the C-terminal coiled-coil region (Fig. 1), which theoretically does not affect the interaction of FREE1 with ABA receptors. In addition, FREE1( $\Delta$ FYVE), which failed to recover the lethality of the *free1* loss-of-function mutant due to defect in MVB biogenesis, was able to complement the ABA-hypersensitive phenotype of *free1-ctmut* (Fig. 1 and Supplementary Fig. 2). Thus, these data reasonably indicated that the ABA hypersensitivity of *free1-ctmut* was less likely caused by defect of MVB-mediated vacuolar sorting and degradation of ABA receptors. As expected, *free1-ctmut* showed no obvious defect in MVB biogenesis at the ultrastructural level and had no increase in the amount of ubiquitinated membrane cargoes<sup>18</sup> (Supplementary Fig. 3). In addition, *free1-ctmut* displayed no obvious defects in both lytic vacuole and protein storage vacuole biogenesis and had no defects in the accumulation of autophagic bodies inside the vacuole upon autophagic induction (Supplementary Fig. 4). To further check whether FREE1-CTmut affects vacuolar sorting and degradation of ABA receptors, we crossed the previously established transgenic plant expressing GFP-PYL4 with the *free1-ctmut* plant and got the double-homozygous line<sup>18</sup>. In the immunoblotting analysis, we did not see an obvious enhancement in the total or ubiquitinated levels of GFP-PYL4 protein (Supplementary Fig. 3). In summary, we conclude that FREE1-CTmut functions normally as an ESCRT component and FREE1 negatively regulates ABA response through the C terminus via an unknown mechanism that is different from the previously reported function of FREE1 in regulating the endosomal sorting of ABA receptors<sup>18</sup>.

## ABA promotes FREE1 nuclear import and nuclear-localized FREE1 complements *free1-ctmut* hypersensitivity to ABA.

The above observation of a possible non-endosomal function of FREE1-CTmut in the regulation of plant response to ABA motivated us to further explore the molecular mechanism behind it. The unobvious change in the expression level of *FREE1* in response to exogenous ABA treatment indicates that the incorporation of FREE1 function in ABA signalling might be at the post-transcriptional level (Supplementary Fig. 1c). Thus, we observed the FREE1 subcellular localization patterns in response to ABA using the previously established GFP-FREE1/*free1* complementary line<sup>8,9,12</sup>. Interestingly, ABA treatment resulted in a significant increase in the level of GFP-FREE1 in the nucleus observed under confocal microscope and detected in the immunoblotting analysis (Fig. 2a,b and Supplementary Fig. 5). In addition, the increase in the level of endogenous FREE1 in the nuclear fraction in WT plants in response to ABA further supports the conclusion that ABA promotes the nuclear import of FREE1 (Fig. 2c). Interestingly, no significant increase in the level of GFP-FREE1-CTmut in the nucleus in response to ABA treatment was observed in the GFP-FREE1-CTmut/*free1-ctmut* line (Fig. 2d). Moreover, immunoblotting analysis with FREE1 antibody further confirmed that the endogenous

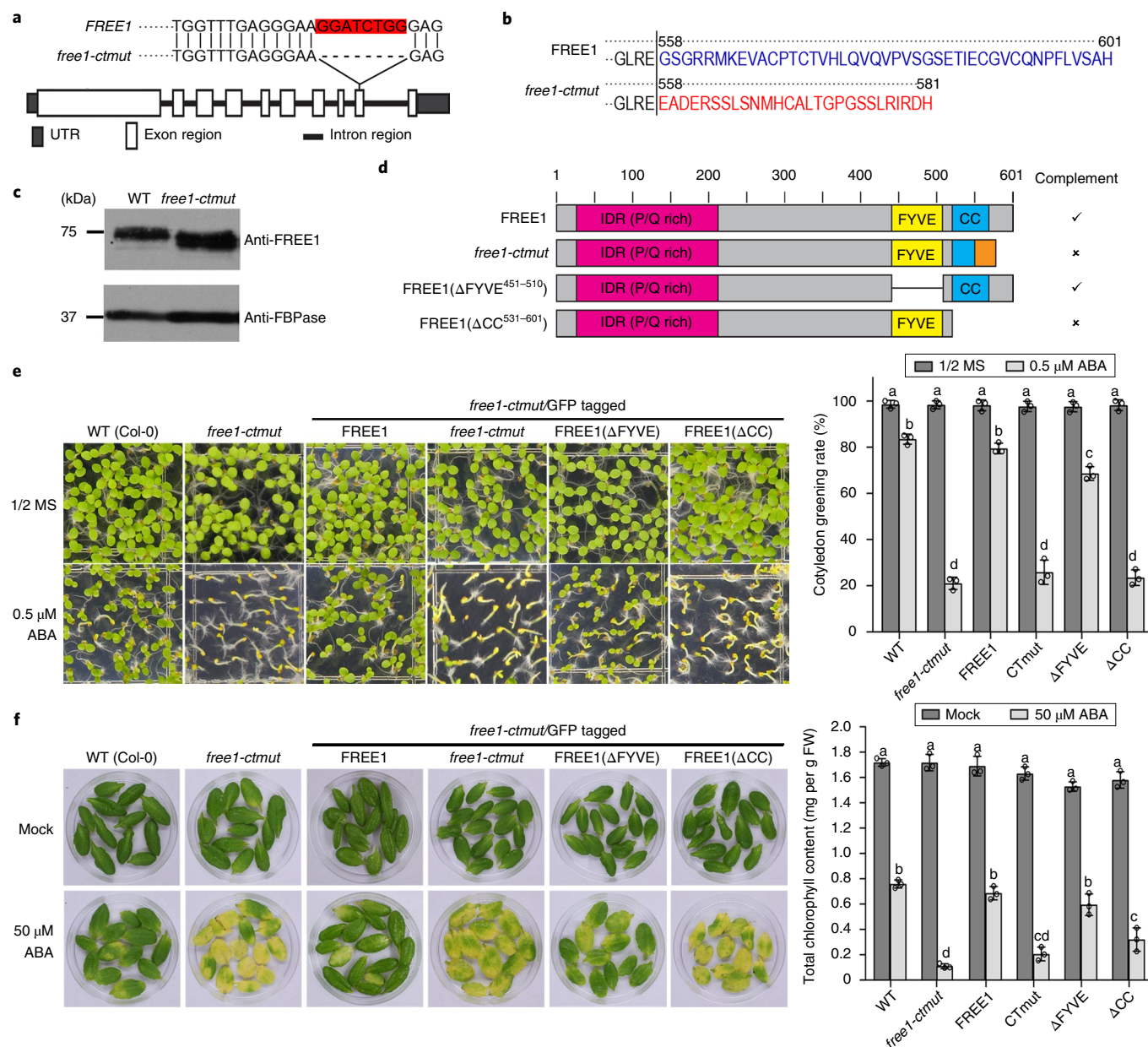


**Fig. 1 | *free1-ctmut* is a newly identified *free1* weak allele and is hypersensitive to ABA treatment. **a–c**, *free1-ctmut* harbours a deletion of eight nucleotides in the ninth exon region (**a**), which leads to a change in amino acids or deletion from 558 to 601 in the C terminus of FREE1 (**b**), and a small reduction in protein size (**c**). FBPase, fructose 1,6-bisphosphatase; UTR, untranslated region. **d**, Various constructs with domain deletions or mutations of FREE1 used for complementation of the *free1-ctmut* plant. CC, coiled coil; IDR, intrinsically disordered region. **e**, Phenotype of Col-0 WT, the *free1-ctmut* mutant and various complemented lines grown on 1/2× MS medium either lacking or supplemented with 0.5 μM ABA (left panel), and quantification of the percentages of the cotyledon greening rate in the indicated backgrounds (right panel). Data are presented as means ± s.e. ( $n=3$  biological replicates). For each biological replicate, around 150 seeds of each genotype were used for seedling establishment assay. **f**, *free1-ctmut* shows enhanced ABA-induced senescence. The detached rosette leaves of 3-week-old plants were incubated under continuous dark in distilled water (mock) or 50 μM ABA for 3 d followed by photographing (left panel) and quantification of the chlorophyll contents (right panel). FW, fresh weight. Data are presented as means ± s.e. ( $n=3$  biological replicates). The different letters above each bar in the right panels of **e** and **f** indicate statistically significant differences as determined by a one-way ANOVA test followed by Tukey's multiple test ( $P < 0.05$ ). The experiment in **c** was performed independently three times with similar results.**

FREE1-CTmut protein failed to translocate into the nucleus in response to ABA (Fig. 2e). These results suggest that FREE1 might exert its inhibitory role in ABA signalling through its action in the nucleus, and the C terminus of FREE1 is essential for its shuttling to the nucleus and plant growth in response to ABA. Then, we suspected that the increase in the level of FREE1 in the nucleus may be able to complement the ABA hypersensitivity phenotype of *free1-ctmut*. The FREE1 protein does not have an obvious nuclear import

signal (NLS) but contains a potential nuclear export signal (NES) in the coding region from 338 to 343 amino acids (LDGLRM). Thus, to increase the levels of FREE1 in the nucleus, we generated the GFP-FREE1-NLS/*free1-ctmut* and GFP-FREE1-NES(mut)/*free1-ctmut* transgenic lines. GFP-FREE1-NLS showed a dominant localization to the nucleus, whereas GFP-FREE1-NES(mut) (L338A/L341A/M343A) showed an obvious increase in nuclear localization without ABA treatment (Fig. 2f). Further phenotypic analysis showed

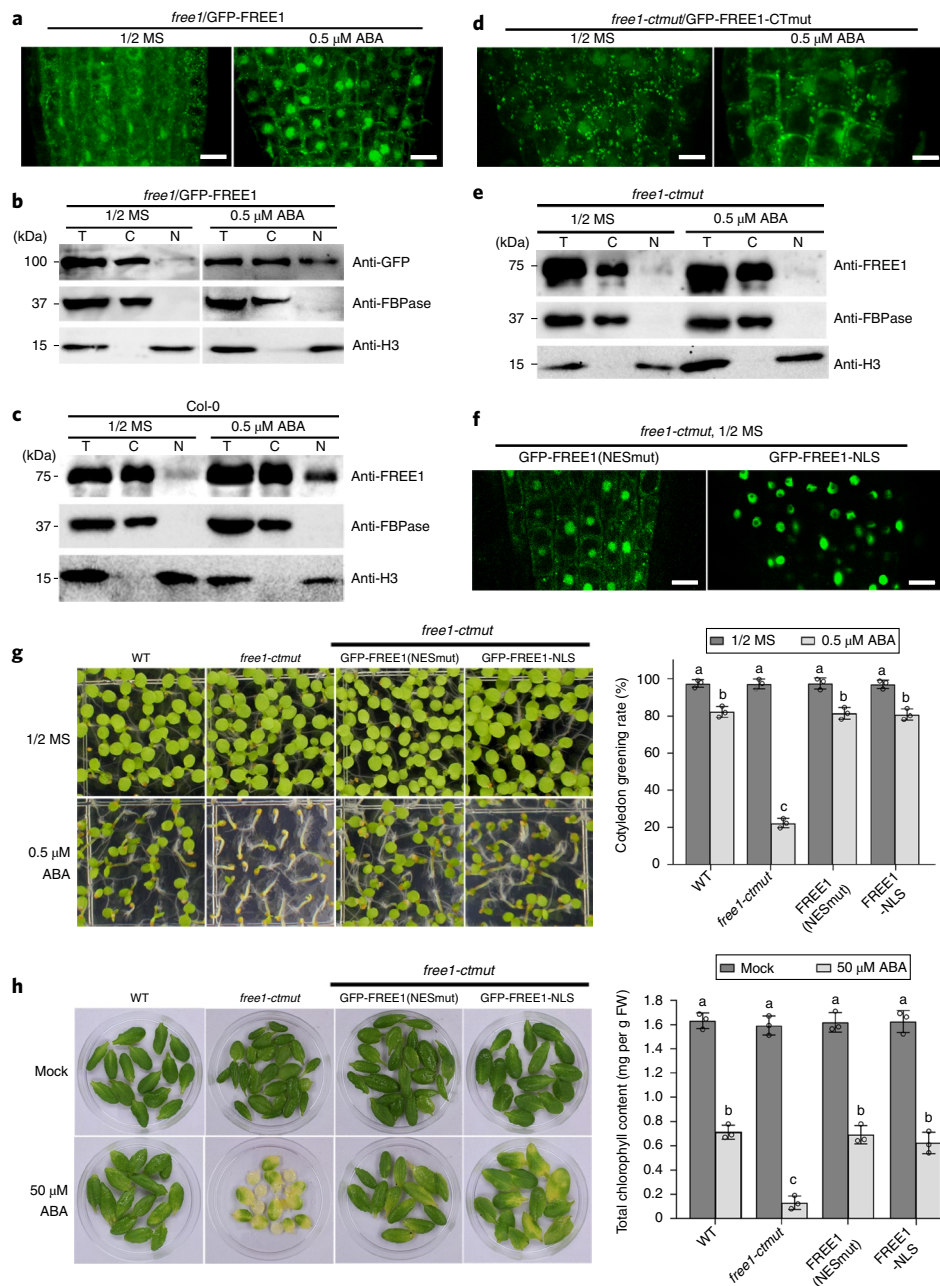


**Fig. 2 | ABA treatment induces nuclear shuttling of FREE1.** **a**, Confocal images of GFP-FREE1 expressed in the roots of the *free1* background grown for 6 d on 1/2 $\times$  MS medium with or without 0.5  $\mu$ M ABA. Scale bars, 10  $\mu$ m. **b,c**, Immunoblot analysis of FREE1 protein distributions in the cytosolic and nuclear fractions. Total (T), cytosol (C) and nuclear (N) proteins were extracted from the *free1*/GFP-FREE1 complemented lines (**b**) and the Col-0 WT plant (**c**) grown for 6 d on 1/2 $\times$  MS medium either lacking or supplemented with ABA, followed by immunoblotting analysis with the indicated antibodies. Anti-FBPase and anti-H3 antibodies were used as protein markers for the cytosolic and nuclear fractions, respectively. **d**, Confocal images of YFP-FREE1-CTmut expressed in *free1-ctmut* grown for 6 d on 1/2 $\times$  MS medium with or without ABA. Scale bars, 10  $\mu$ m. **e**, Immunoblotting analysis of the FREE1 protein distribution in cytosolic and nuclear fractions extracted from the plants shown in **d**. **f**, GFP-FREE1(NESmut) and GFP-FREE1-NLS were largely localized to the nucleus when expressed in *free1-ctmut* grown for 6 d on 1/2 $\times$  MS medium. Scale bars, 10  $\mu$ m. **g**, GFP-FREE1(NESmut) and GFP-FREE1-NLS complement the ABA-responsive phenotype of *free1-ctmut*. The indicated plants were grown for 6 d on 1/2 $\times$  MS medium either lacking or supplemented with 0.5  $\mu$ M ABA (left panel), and quantification of the percentage of seedling establishment is shown (right panel). **h**, The detached rosette leaves were incubated under continuous dark in 50  $\mu$ M ABA or distilled water (mock) for 3 d followed by photographing (left panel) and quantification of the chlorophyll contents (right panel). Data in the right panels of **g** and **h** are presented as means  $\pm$  s.e. ( $n = 3$  biological replicates). The different letters above each bar indicate statistically significant differences as determined by one-way ANOVA analysis followed by Tukey's multiple test ( $P < 0.05$ ). The experiments in **a-f** were repeated independently three times with similar outcomes obtained.

that both GFP-FREE1-NLS and GFP-FREE1-NES(mut) were able to complement the *free1-ctmut* hypersensitivity phenotype to ABA (Fig. 2g,h and Supplementary Fig. 6). Taken together, we conclude

that ABA treatment promotes nuclear accumulation of FREE1 but not FREE1-CTmut, and nuclear accumulation of FREE1 is able to complement the *free1-ctmut* hypersensitivity phenotype to ABA.

**ABA promotes FREE1 phosphorylation and phosphorylated FREE1 is mainly located in the nucleus.** Numerous studies have shown that phosphorylation modification modulates protein nucleocytoplasmic shuttling. We reasonably suspect that FREE1 may be subjected to phosphorylation modification when treated with ABA. To test this hypothesis, we detected the phosphorylation level of FREE1 with or without ABA treatment, and the results showed that ABA treatment dramatically increased the phosphorylation level of FREE1 (Fig. 3a). To know whether the C-terminal is required for ABA-induced FREE1 phosphorylation, we detected the phosphorylation level of FREE1-CTmut in the GFP-FREE1-CTmut/*free1-ctmut* line. The results showed that the increase in the level of FREE1-CTmut phosphorylation was much less than that of FREE1 (Fig. 3a), suggesting that the C-terminal is required for ABA-induced FREE1 phosphorylation. Next, we asked whether the FREE1 phosphorylation correlated with FREE1 nuclear import, and detected the FREE1 phosphorylation level with or without ABA treatment in both nuclear and cytosolic fractions. The results showed that phosphorylated FREE1 was mainly located in the nucleus (Fig. 3b), indicating that FREE1 may require a phosphorylation modification for its accumulation in the nucleus. Further time course and dose-response experiments were performed to examine the efficiency and the potency of ABA-induced FREE1 phosphorylation. Direct treatment of the plants by submergence of the seedlings in liquid medium containing 40  $\mu$ M ABA was able to induce the obvious increase in the levels of FREE1 phosphorylation at 1 h after treatment, whereas transferring the seedlings to an ABA agar plate induced FREE1 phosphorylation at later time (Supplementary Fig. 7). For the dosage assay, a concentration of 10  $\mu$ M ABA is able to induce FREE1 phosphorylation 48 h after transferring to agar plates containing ABA (Supplementary Fig. 7). Taken together, we concluded that ABA was able to induce FREE1 phosphorylation, which required the C-terminal of FREE1, and phosphorylated FREE1 was mainly located in the nucleus.

**SnRK2.2/2.3-dependent phosphorylation of FREE1 is necessary for ABA-induced FREE1 nuclear import.** Many studies have shown that SnRK2 clade protein kinases, including SnRK2.2, SnRK2.3 and SnRK2.6, are key positive regulators mediating plant response to ABA, which are strongly activated by ABA for further phosphorylation of downstream factors<sup>26</sup>. To test whether SnRK2 kinases phosphorylate FREE1 in response to ABA, we first tested the interactions between SnRK2s and FREE1. The yeast two-hybrid results showed that FREE1 directly interacted with SnRK2.2 and SnRK2.3, but not with SnRK2.6 (Supplementary Fig. 8). Further bimolecular fluorescence complementation (BiFC) assays verified the interaction of FREE1 with SnRK2.2/2.3 in both the nucleus and the cytosol in *Arabidopsis* leaf protoplasts (Fig. 3c and Supplementary Fig. 8). The co-immunoprecipitation data showed that ABA treatment enhanced the association between FREE1 with either SnRK2.2 and SnRK2.3 (Fig. 3d). To clarify the domain in FREE1 that is required for interaction with SnRK2.2 and SnRK2.3, we next generated several FREE1 mutants harbouring domain truncations for interaction analysis with SnRK2s. As shown in Supplementary Fig. 8, deletion of the C terminus harbouring the coiled-coil domain, but not the FYVE domain or the large N-terminal part (1–420), abolished the interaction between FREE1 and SnRK2s. Thus, the C-terminal coiled-coil region of FREE1 was responsible for the interaction with SnRK2.2 and SnRK2.3.

The direct interactions between FREE1 and SnRK2.2 or SnRK2.3 strongly suggest that SnRK2 kinases may phosphorylate FREE1 in response to ABA. To further prove this hypothesis, we co-expressed GFP-FREE1 with either yellow fluorescent protein-tagged SnRK2.2 (YFP-SnRK2.2) or YFP-SnRK2.3 in *Arabidopsis* leaf protoplasts to detect the FREE1 phosphorylation status with or without ABA treatment. The results showed that, upon ABA treat-

ment, co-expression with either YFP-SnRK2.2 or YFP-SnRK2.3 resulted in a significant enhancement of FREE1 phosphorylation (Supplementary Fig. 9). We next performed an in vitro phosphorylation assay to test whether SnRK2 kinases directly phosphorylate FREE1. Purified His-Sumo-FREE1 was incubated with either the immunoprecipitated GFP-SnRK2 proteins from ABA-treated transgenic plants or the purified His-MBP-SnRK2 from *Escherichia coli*. Phosphorylation of His-Sumo-FREE1 was readily detectable in both cases (Fig. 3e and Supplementary Fig. 10). In addition, we also noticed that, in comparison with the ABA-activated GFP-SnRK2, much more His-MBP-SnRK2 proteins were needed in the in vitro reaction to induce the phosphorylation of His-Sumo-FREE1 (Fig. 3e and Supplementary Fig. 10), which is consistent with the previous reports that the *E. coli*-expressed SnRK2.2 and SnRK2.3 have low kinase activities<sup>27,28</sup>. The above in vivo and in vitro experimental results suggested that SnRK2.2 and SnRK2.3 represent the expected kinase proteins responsible for ABA-induced FREE1 phosphorylation. To further reveal that if ABA-induced and SnRK2s-dependent phosphorylation of FREE1 is responsible for ABA-induced FREE1 nuclear import, we introduced GFP-FREE1 into the leaf protoplasts derived from available *snrk2.2/2.3/2.6* triple mutants, and no obvious increase of FREE1 nuclear import was observed in *snrk2.2/2.3/2.6* protoplasts upon ABA treatment (Fig. 3f). This observation was fostered by the immunoblotting evidence that no obvious increase in the levels of endogenous FREE1 in the nuclear fraction was detected in *snrk2.2/2.3/2.6* triple mutants upon ABA treatment (Fig. 3g). Collectively, these results suggest that SnRK2.2-dependent and SnRK2.3-dependent phosphorylation of FREE1 is necessary for ABA-induced FREE1 nuclear import.

**Phosphorylations at serine residues S530/S533 are required for ABA-induced FREE1 nuclear import.** To identify the corresponding FREE1 phosphorylation residues in response to ABA, we performed mass spectrometry analysis on the immunoprecipitated GFP-FREE1 and GFP-FREE1-CTmut proteins enriched from ABA-treated complement plants. Six phosphorylated residues were detected by immunoprecipitation–mass spectrometry analysis (Supplementary Fig. 11), and two phosphorylation sites, S530 and S533, located in the FREE1 C-terminal coiled-coil region, were less detectable in the GFP-FREE1-CTmut protein. The deletion in the FREE1-CTmut protein probably disrupts the structure of the coiled-coil region, which might reduce phosphorylation of S530 and S533. Thus, we focused our current study on the functional characterization of S530 and S533 in conferring ABA responses.

To further verify whether phosphorylation of S530 and S533 contributes to the ABA-induced FREE1 nuclear import, we introduced YFP-FREE1(S530A/S533A) and YFP-FREE1(S530D/S533D), in which these two serine sites were mutated into non-phosphorylatable alanine or phosphorylation-mimicking aspartic acid residues, into the *free1-ctmut* mutant for FREE1 localization observation and plant phenotypic analysis in response to ABA. No obvious accumulation of YFP-FREE1(S530A/S533A) in the nucleus was detected in both confocal observation and immunoblotting analysis of different protein fractions in the plants with and without ABA treatment (Fig. 4b,c). On the contrary, YFP-FREE1(S530D/S533D) showed an obvious nuclear accumulation in the complemented plants even without ABA treatment (Fig. 4d,e). In addition, consistent with the immunoprecipitation–mass spectrometry result, phosphorylation levels of YFP-FREE1(S530A/S533A) in ABA-treated transgenic plants and the purified His-Sumo-FREE1(S530A/S533A) in the in vitro phosphorylation assay were both obviously decreased (Figs. 3e and 4f and Supplementary Fig. 10). YFP-FREE1(S530A/S533A)/*free1-ctmut* showed similar ABA hypersensitivity as *free1-ctmut*, whereas YFP-FREE1(S530D/S533D)/*free1-ctmut* resembled the WT in terms of seedling establishment as well as ABA-induced

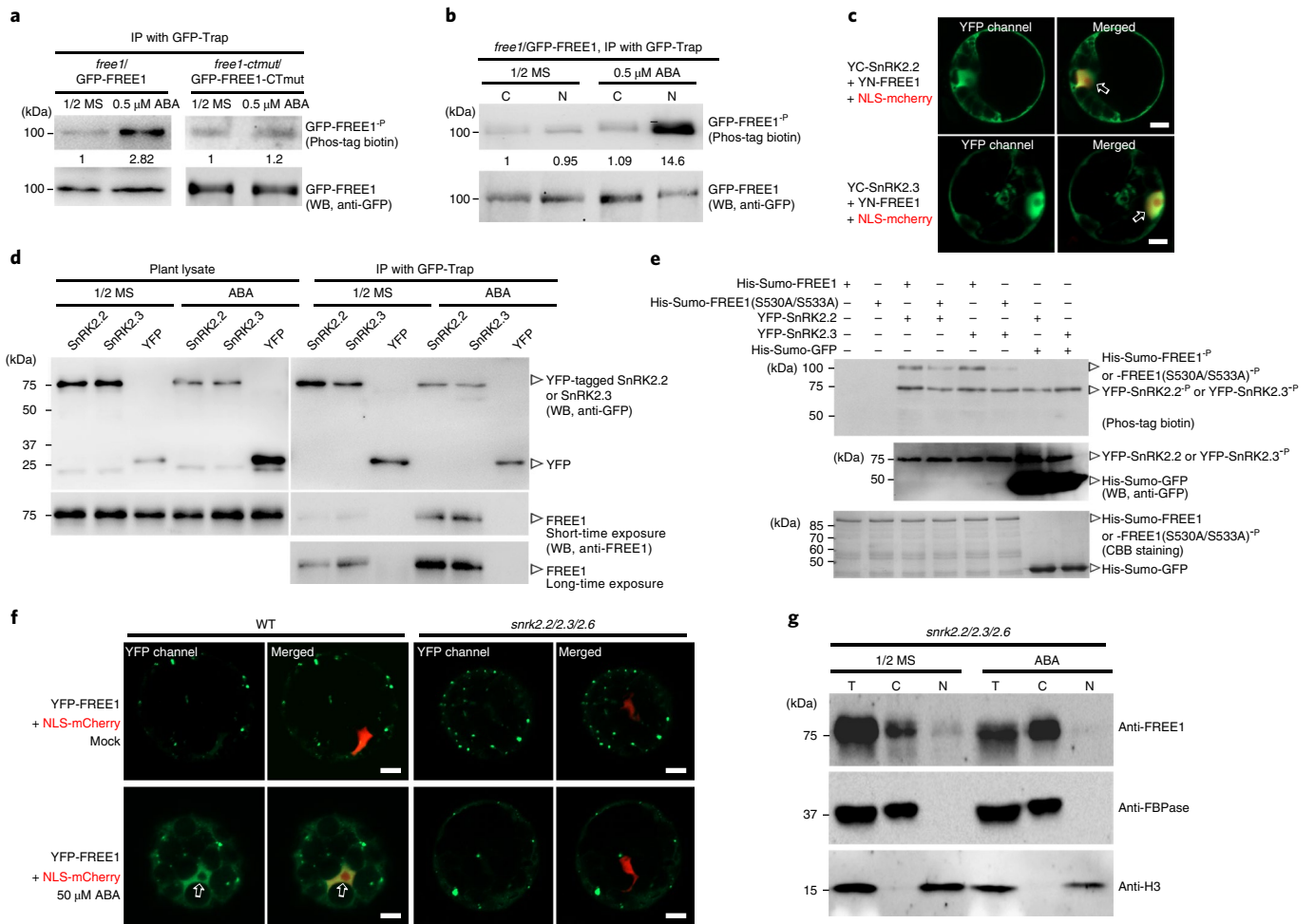


**Fig. 3 | SnRK2 kinases interact with and phosphorylate the FREE1 protein.** **a**, ABA treatment increases the phosphorylation level of FREE1 but not FREE1-CTmut. To analyse FREE1 phosphorylation, proteins were extracted from the indicated complemented lines grown on the medium either lacking or supplemented with 0.5  $\mu\text{M}$  ABA, followed by immunoprecipitation (IP) with GFP-Trap. The same amount of immunoprecipitated proteins from each sample was used for detection with either phos-tag BTL-111 or anti-GFP antibody. The relative intensities of each band detected with phos-tag and anti-GFP were quantified using ImageJ and the first lane in each experiment was arbitrarily set to 1. **b**, To dissect the cellular distribution of phosphorylated FREE1, proteins from cytosolic and nuclear fractions were used for immunoprecipitation with GFP-Trap, followed by phosphorylation detection. In **a** and **b**, the numbers between the bands indicate the phosphorylated/non-phosphorylated ratio. **c**, BiFC assays confirm the interactions of FREE1 and SnRK2 kinases in *Arabidopsis* protoplasts. NLS-mCherry was co-expressed as a nuclear marker. The arrows indicate the nucleus. Scale bars, 10  $\mu\text{m}$ . **d**, Co-immunoprecipitation assays demonstrate the interactions between FREE1 and SnRK2.2 or SnRK2.3. Proteins were extracted from GFP, YFP-SnRK2.2 or YFP-SnRK2.3 transgenic plants grown on the medium either lacking or supplemented with 0.5  $\mu\text{M}$  ABA, followed by immunoprecipitation with GFP-Trap and detection with the indicated antibodies. **e**, SnRK2 kinases phosphorylate FREE1 in vitro. Immunoprecipitated YFP-SnRK2.2 and YFP-SnRK2.3 proteins were incubated with purified His-Sumo-FREE1, His-Sumo-FREE1(S530A/S533A) or His-Sumo-GFP in phosphorylation buffer, followed by SDS-PAGE separation and visualization with Coomassie brilliant blue (CBB) staining, or detection with phos-tag BTL-111 and anti-GFP antibody. **f**, YFP-FREE1 was expressed in *Arabidopsis* protoplasts derived from WT or the *snrk2.2/2.3/2.6* mutant, followed by 50  $\mu\text{M}$  ABA treatment and confocal observation. The arrows indicate the nucleus. Scale bars, 10  $\mu\text{m}$ . **g**, Immunoblot analysis of FREE1 protein distribution in the *snrk2.2/2.3/2.6* mutant grown for 6 d on 1/2x MS medium either lacking or supplemented with 0.5  $\mu\text{M}$  ABA. The experiments in **a-g** were repeated independently three times with similar results.

leaf senescence (Fig. 4g,h and Supplementary Fig. 6), further supporting that phosphorylations at S530/S533 are essential for FREE1 function in the nucleus in response to ABA.

**FREE1 represses ABF4 and ABI5 transcription activity through inhibition of their DNA-binding abilities.** To investigate FREE1 function in the nucleus in response to ABA, we performed a yeast two-hybrid screening in the *Arabidopsis* complementary DNA library using the C-terminal part of FREE1(231–601) as bait; the full-length FREE1 protein was not used as a bait for screening owing to its high self-activation activity. In the positive colonies, we identified the clones that encode the transcriptional activators

ABF4 and ABI5. The genes encoding these two proteins were cloned for further protein interaction analysis. Indeed, both ABF4 and ABI5 interacted with FREE1(231–601) in the yeast two-hybrid assay (Fig. 5a and Supplementary Fig. 12). We also cloned other ABA-responsive transcription factors, such as ABF1, ABF2, ABF3 and ABI4, but failed to detect their interactions with FREE1 in the yeast two-hybrid analyses (Supplementary Fig. 12). The interactions of FREE1 with either ABF4 or ABI5 in the nucleus were further confirmed by the BiFC assay (Fig. 5b and Supplementary Fig. 12). Further fine-mapping in the yeast two-hybrid assays showed that FREE1-CTmut(231–581) lost interactions with both ABF4 and ABI5, whereas FREE1(421–601) with a deletion of the large

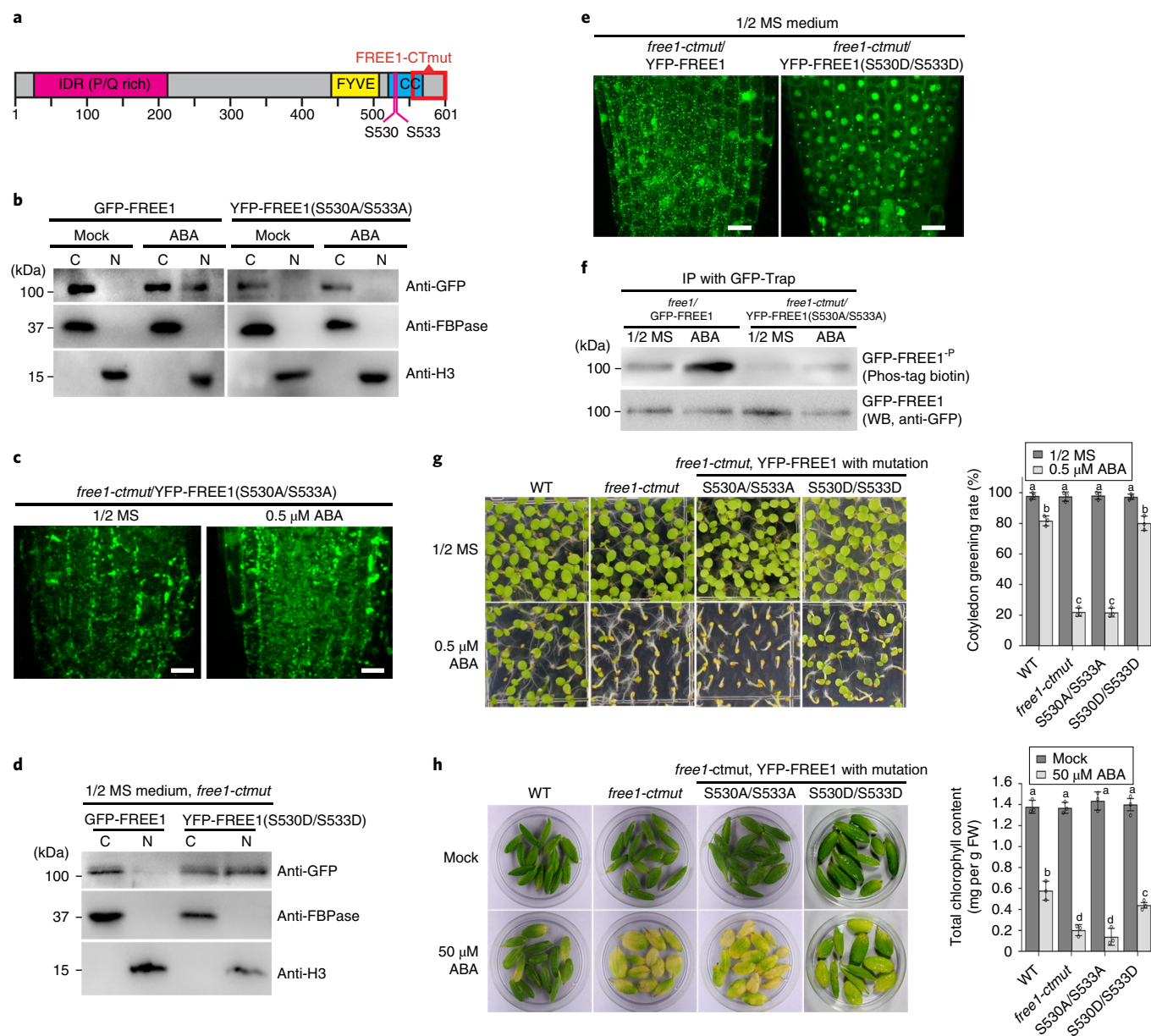


**Fig. 4 | Identification of the phosphorylation sites located in the C terminus of FREE1.** **a**, Mass spectrometry identification of two phosphorylation sites, S530 and S533, located in the coiled-coil region of the FREE1 protein. **b**, Immunoblot analysis of GFP-FREE1 or YFP-FREE1(S530A/S533A) proteins in the cytosolic and nuclear fractions extracted from the cells with or without ABA treatment. **c**, Confocal microscopic images of *free1-ctmut*/YFP-FREE1(S530A/S533A) plants grown for 6 d on 1/2 MSx medium either lacking or supplemented with 0.5  $\mu$ M ABA. Scale bars, 10  $\mu$ m. **d**, Immunoblot analysis of GFP-FREE1 or YFP-FREE1(S530D/S533D) proteins in the cytosolic and nuclear fractions extracted from the indicated plants without ABA treatment. **e**, Confocal microscopic images of the indicated plants grown for 6 d on 1/2x MS medium. Scale bars, 10  $\mu$ m. **f**, The YFP-FREE1(S530A/S533A) mutant shows a reduced phosphorylation level following ABA treatment. Total proteins were extracted from the indicated plants grown for 6 d on 1/2x MS medium either lacking or supplemented with 0.5  $\mu$ M ABA, and were used for immunoprecipitation with GFP-Trap followed by phosphorylation detection. **g,h**, YFP-FREE1(S530D/S533D) but not FREE1(S530A/S533A) could complement the *free1-ctmut* phenotype. Seedlings of the indicated genotypes were grown on 1/2x MS or 1/2x MS plus 0.5  $\mu$ M ABA for 6 d followed by photographing and quantification of the cotyledon greening rate (**g**). Detached rosette leaves of 3-week-old plants were incubated under continuous dark in 50  $\mu$ M ABA or distilled water (mock) for 3 d followed by photographing and quantification of the chlorophyll contents (**h**). Data in **g** and **h** are presented as means  $\pm$  s.e. ( $n=3$  biological replicates). The different letters above each bar indicate statistically significant differences as determined by a one-way ANOVA test followed by Tukey's multiple test ( $P < 0.05$ ). The experiments in **b-f** were repeated independently three times with similar results.

N-terminal part could still interact with these transcription factors (Supplementary Fig. 12). Collectively, these results demonstrated that the C-terminal-located coiled-coil domain of FREE1 was specifically responsible for the interaction with the DNA-binding domains of ABF4 and ABI5 (Fig. 5a and Supplementary Fig. 12).

Intriguingly, we found that FREE1(S530A/S533A) abolished the interactions of FREE1 with ABF4 and ABI5 (Supplementary Fig. 12), indicating the phosphorylation-dependent interactions between FREE1 and the ABA-responsive transcription factors. Indeed, the co-immunoprecipitation assay showed that, in the absence of ABA,

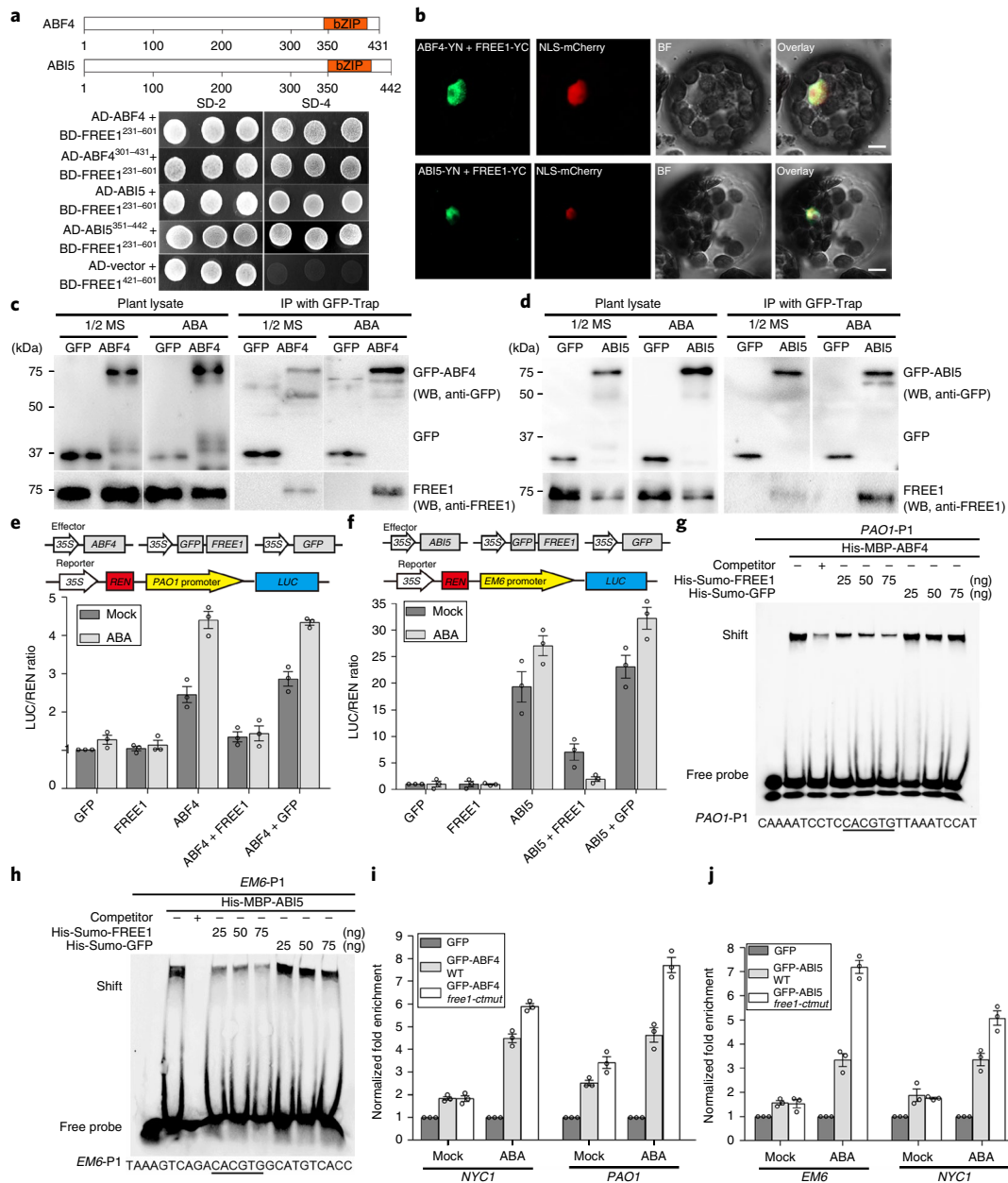


**Fig. 5 | FREE1 interacts with and suppresses the transcriptional activation activities of ABF4 and ABI5.** **a**, Domain structures of the ABF4 and ABI5 proteins (top panel) and yeast two-hybrid analysis of the binary interactions between FREE1 and ABF4 or ABI5 (bottom panel). The three dots mean that three different colonies were picked for the interaction assay. bZIP, basic leucine zipper. **b**, The BiFC assay shows that FREE1 interacts with ABF4 and ABI5 in the nucleus. Scale bar, 10  $\mu$ m. BF, bright field. **c,d**, ABA treatment increases the interactions between FREE1 and ABF4 or ABI5. Proteins were extracted from 35Spro::GFP, GFP-ABF4 (**c**) or GFP-ABI5 (**d**) transgenic plants grown on the medium either lacking or supplemented with 0.5  $\mu$ M ABA, followed by immunoprecipitation with GFP-Trap and immunoblotting with the indicated antibodies. **e,f**, The dual-luciferase reporter assay shows that the transcriptional activation activities of ABF4 (**e**) and ABI5 (**f**) are repressed by FREE1. The top panel shows the schematic structures of the reporter and effector constructs used in the dual-luciferase reporter assay. Data in **e** and **f** are presented as means  $\pm$  s.e. ( $n=3$  biological replicates). **g,h**, Gel-shift assays (EMSA) show that FREE1 inhibits the DNA-binding activities of ABF4 (**g**) and ABI5 (**h**). His-Sumo-FREE1, His-Sumo-GFP, His-MBP-ABF4 and His-MBP-ABI5 recombinant proteins were subjected to the EMSA assay according to the procedures described in the Methods. Underlined text indicates the G-box *cis*-element recognized by ABF4 and ABI5 transcription factors. **i,j**, ChIP-qPCR assays demonstrate enriched binding of *cis* elements of downstream genes to the transcription factors ABF4 (**i**) and ABI5 (**j**) in *free1-ctmut* following ABA treatment. Seedlings of 6-day-old plants grown on 1/2x MS medium either lacking or supplemented with 0.5  $\mu$ M ABA were used for ChIP-qPCR analysis. The level of binding was calculated as the ratio between immunoprecipitation and input. The GFP control set was arbitrarily set to 1. Data in **i** and **j** are presented as means  $\pm$  s.e. ( $n=3$  technical replicates). The experiments in **i** and **j** were repeated twice with similar results. The experiments in **a-d**, **g** and **h** were repeated independently three times with similar outcomes obtained.

the interactions between FREE1 and ABF4 or ABI5 were weak, but were enhanced upon ABA treatment (Fig. 5c,d). In addition, we found that, in contrast to GFP-FREE1-NLS, the nuclear-located

GFP-FREE1-CTmut-NLS was not able to complement the *free1-ctmut* hypersensitivity phenotype to ABA in terms of seedling establishment (Supplementary Fig. 13). These results indicate the

essential role of phosphorylation of FREE1 C-terminal residues in the regulation of the ABA response.

The specific interactions of FREE1 with the DNA-binding domains of ABF4 and ABI5 prompted us to test whether FREE1 affects the transcriptional activation activities of these two transcription factors in plant cells. First, we employed a widely used dual-luciferase-based reporter assay in *Arabidopsis* protoplasts. The results showed that ABA dramatically induced the expression of *PAO1* or *EM6* in the presence of ABF4 or ABI5, individually, and this induction was significantly inhibited when co-expressed with GFP-FREE1, but not with the GFP control (Fig. 5e,f and Supplementary Fig. 12), suggesting a direct inhibition of FREE1 towards the transcriptional activation activities of ABF4 and ABI5 in response to ABA. Next, to test whether FREE1 inhibits ABF4 and ABI5 transcriptional activation activities through competitive binding to the DNA-binding domains of these two transcription factors, we investigated the effect of FREE1 on the binding activities of these two transcription factors to the *cis*-regulatory sequences of downstream genes by performing an electrophoretic mobility shift assay (EMSA). The results showed that FREE1, but not the GFP control, inhibits the DNA-binding abilities of ABF4 and ABI5 in a dosage-dependent manner (Fig. 5g,h), supporting a direct inhibition effect of FREE1 on the transcriptional activation activities of ABF4 and ABI5. We then sought to further examine whether the *free1-ctmut* mutation would result in an enhanced enrichment of GFP-ABF4 and GFP-ABI5 towards the promoter sequences of their target genes using the chromatin immunoprecipitation–quantitative PCR (ChIP–qPCR) assay, with GFP as a negative control. The results showed that, in response to ABA treatment, significantly increased enrichments of the promoter sequences of downstream genes, including *NYC1*, *PAO1* and *EM6*, for GFP-ABF4 and GFP-ABI5 were detected in the *free1-ctmut* mutant, which suggested that FREE1 indeed attenuated the DNA-binding abilities of ABF4 and ABI5 towards the promoter regions of the downstream target genes (Fig. 5i,j).

**Depletions of ABF4 or ABI5 rescue the ABA hypersensitivity phenotype conferred in the *free1-ctmut* mutant.** It is highly possible that the hypersensitivity phenotype of the *free1-ctmut* mutant to ABA is caused mainly by an overactivation of ABF4 and ABI5 without FREE1 inhibition in the nucleus. To confirm this possibility, we tested whether the depletions of ABF4 or ABI5 would rescue the ABA hypersensitivity phenotypes observed in the *free1-ctmut* mutants by crossing *free1-ctmut* with either *abf4* or *abi5* mutants. Consistent with our expectation, the *abf4* or *abi5* mutation in *free1-ctmut* showed a WT ABA response in terms of both seedling establishment and ABA-induced leaf senescence (Fig. 6a,b), supporting the conclusion that the ABA hypersensitivity phenotype of *free1-ct* is probably caused by an overactivation of the transcriptional activities of ABF4 and ABI5. In addition, we also noticed that *free1-ctmut/abf4* double mutants were more sensitive to ABA than *free1-ctmut/abi5* double mutants under 0.75  $\mu$ M ABA (Supplementary Fig. 14), which is consistent with the more dominant role of ABI5 than of ABF4 as a transcription factor in ABA signalling<sup>16,29</sup>. We next detected the relative expression levels of ABA-responsive genes, including *NYE1*, *NYC1*, *PAO1*, *RD29A*, *RD29B*, *NYE2* and *SAG29* in the WT, the *free1-ct* mutant, *abf4*, *abi5*, *free1-ctmut/abf4* and *free1-ctmut/abi5* with or without ABA treatment. In agreement with our hypothesis, all of the detected genes showed elevated expression in the *free1-ctmut* mutant without ABA treatment, and upon ABA treatment, the rise of expression induction become more prominent. However, the *abf4* or *abi5* mutation eliminated such expression induction of ABA-responsive genes in *free1-ctmut* (Fig. 6c,d). Collectively, these results strongly suggest that the elevated expression of ABA-responsive genes in *free1-ctmut* was caused by overactivation of ABF4 and ABI5 transcriptional activity.

## Discussion

Previous studies have demonstrated the important functions of FREE1 as a component of ESCRT in regulating MVB biogenesis and MVB-mediated endosomal sorting<sup>8,9,12,13</sup>. In this study, we further uncovered a previously unappreciated function of FREE1 in the nucleus as a negative regulator to attenuate ABA signalling. Several lines of cellular, biochemical and genetic evidence strongly support our hypothesis: (1) a portion of the FREE1 protein translocates into the nucleus in response to ABA treatment; (2) SnRK2.2 and SnRK2.3 mediate FREE1 phosphorylation, a prerequisite step for FREE1 nuclear import; (3) phosphorylated FREE1 interacts with ABF4 and ABI5 in the nucleus to inhibit their transcriptional activation activities; (4) the *free1-ct* mutant with defects in nuclear import of FREE1 in response to ABA shows normal growth and vacuolar sorting route, but displays hypersensitivity to ABA treatment; and (5) the *abf4* and *abi5* mutants are epistatic to the *free1-ctmut* in ABA sensitivity. Based on the findings in this study and the previous report about FREE1 function in ABA signalling<sup>18</sup>, we proposed a ‘double-brake’ working model for FREE1 function in attenuation of ABA signalling (Fig. 6e), in which FREE1 can (1) function in the cytoplasm to negatively regulate the cellular protein level of ABA receptors by mediating their vacuolar degradation in an ESCRT-dependent pathway; and (2) translocate into the nucleus to repress the transcription factors ABF4 and ABI5.

Phosphorylation can promote the nuclear import of cargo proteins by affecting the binding affinity of the NLS to importins or inducing a conformational change that exposes the NLS to be accessible to importin<sup>30</sup>. In our current study, SnRK2.2 or SnRK2.3 directly interacts with FREE1 to induce phosphorylation at the serine sites S530 and S533 and nuclear shuttling of FREE1 in response to ABA treatment. The two phosphorylation sites S530 and S533 reside in the C-terminal-located coiled-coil domain of FREE1. Mutations of these two serine residues or disruption of the coiled-coil domain abolished the nuclear import of FREE1 (Figs. 2 and 4). These results highlight the important role of the C-terminal coiled-coil domain in conferring nuclear import of FREE1, although no canonical NLS can be found in the FREE1 protein. It is possible that phosphorylation of the serine residues in the coiled-coil domain may induce the association of FREE1 with other proteins such as 14-3-3 or importins, which have been frequently shown to function as chaperones to mediate nuclear shuttling of cargoes, a process usually accompanied by phosphorylation modification<sup>31–34</sup>. Another possibility is that the phosphorylation modification might cause the conformational change of FREE1, thereby hiding the NES and leading to the promotion of FREE1 accumulation in the nucleus. Indeed, mutation of the NES leads to the accumulation of FREE1 in the nucleus, and NES-mutated FREE1 can function normally in the nucleus to fully recover the ABA hypersensitivity of *free1-ctmut*. Other questions regarding the phosphorylation-dependent nucleocytoplasmic shuttling of FREE1 are how FREE1 exports from the nucleus after termination of ABA signalling and whether a protein dephosphorylation mechanism is involved in FREE1 nuclear export.

The ABA-responsive transcription factors ABI5 and ABF4 function as key regulators in the ABA signalling pathway controlling seed dormancy, germination and plant responses to environmental stresses<sup>29,35,36</sup>. Thus, the activation of these transcription factors must be tightly regulated to avoid inappropriate cellular responses. The ABI5 expression can be activated by itself and can also be positively or negatively regulated by many upstream transcription factors, such as ABI3, ABI4, MYB7 and WRKYs<sup>29,36</sup>. In addition, the stability and activity of ABI5 and ABF4 are also regulated through a combination of different post-translational modifications, such as phosphorylation, ubiquitylation and SUMOylation<sup>16</sup>. Here, we identified FREE1 as a new repressor in inhibiting the transcriptional activation activities of ABI5 and ABF4. Our results showed that FREE1 directly interacts with the DNA-binding domains of these

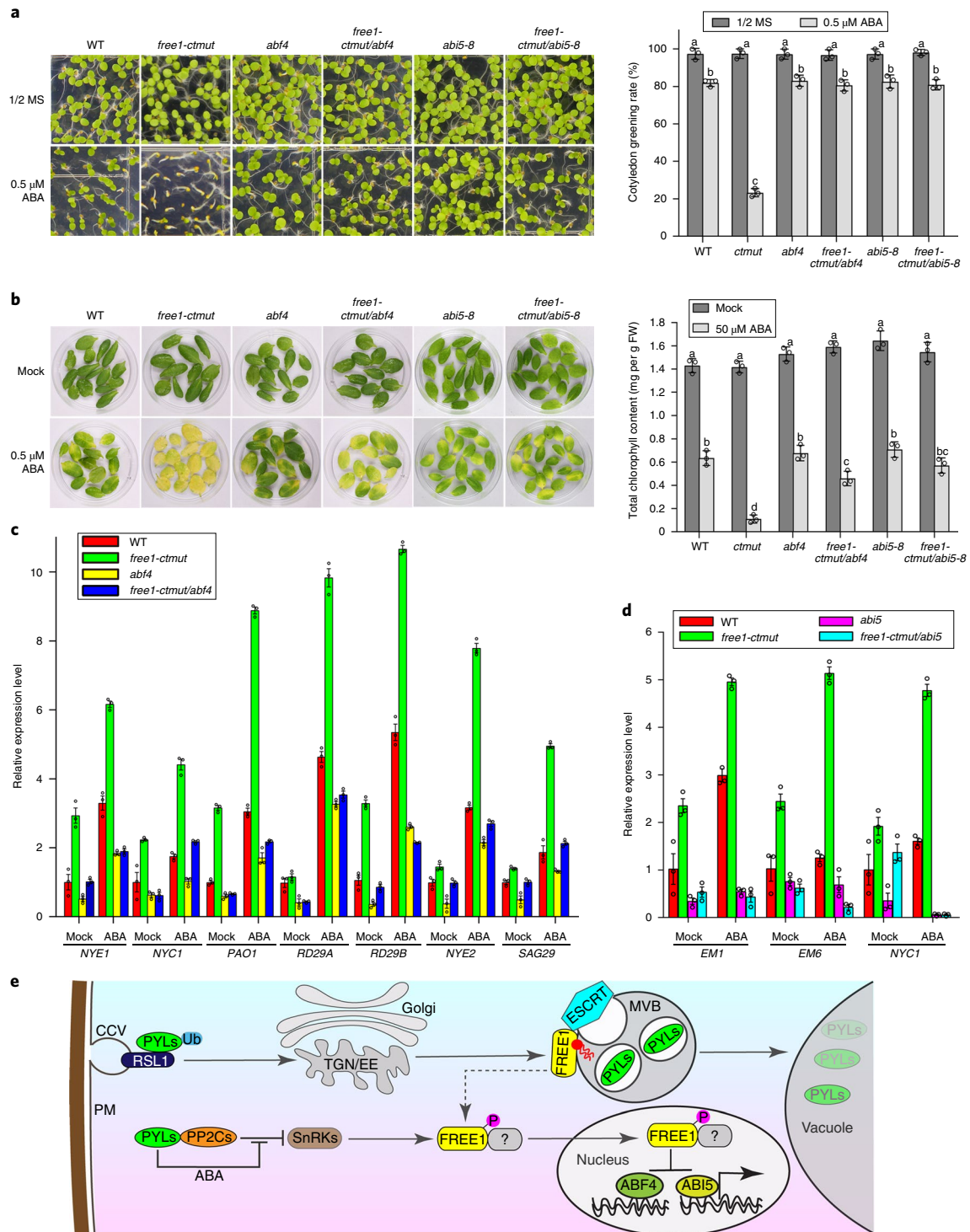


**Fig. 6 | Genetic interactions between FREE1 and ABF4 or ABI5. a**, Photographs of the plants in the indicated backgrounds grown for 6 d on 1/2× MS medium either lacking or supplemented with 0.5 μM ABA (left panel) and quantification of the percentages of the cotyledon greening rate (right panel). **b**, Photographs of the detached rosette leaves incubated under continuous dark in 50 μM ABA or distilled water (mock) for 3 d (left panel) and quantification of the chlorophyll contents (right panel). Data in **a** and **b** are presented as means ± s.e. ( $n = 3$  biological replicates). The different letters above each bar indicate statistically significant differences as determined by one-way ANOVA analysis followed by Tukey's multiple test ( $P < 0.05$ ). **c, d**, qRT-PCR quantification of the transcript levels of various ABA-responsive genes in the indicated plants. The Col-0 WT, *free1-ctmut*, *abf4*, *free1-ctmut/abf4* and *free1-ctmut/abi5* plants grown for 5 d were transferred to liquid medium supplemented with or without 40 μM ABA for 1 h, followed by RNA extraction and qRT-PCR analysis. The transcript levels of these indicated genes in untreated Col-0 plants were arbitrarily set to 1. *UBQ10* was used as a reference. Data in **c** and **d** are presented as means ± s.e. ( $n = 3$  biological replicates). **e**, The working model of FREE1 in ABA signalling. A 'double-brake' working model of FREE1 functions in plant ABA signalling (see the Discussion section). The question marks indicate the unknown factors that are presumably involved in cytosol-nuclear shuttling of FREE1. The dashed arrow indicates a portion of MVB-localized FREE1 that may be subjected to phosphorylation. CCV, clathrin-coated vesicle; EE, early endosome; PM, plasma membrane; TGN, trans-Golgi network; Ub, ubiquitin.

transcription factors and competitively affects their binding to the *cis*-element regulatory sequences of the downstream genes. FREE1 interacts with both ABF4 and ABI5 with their respective basic leucine zipper-type DNA-binding domain, suggesting the possible existence of a broad repression regulation of FREE1 towards a group of transcription factors sharing structure similarities. The FREE1 protein has no obvious DNA-binding domain and does not have a known domain similar to the reported sequences that possess transcription repressor activity; thus, it is unknown how FREE1 exactly inhibits the transcriptional regulation activities of ABF4 and ABI5. Studies have shown that in eukaryotic cells, transcriptional repressors function mainly through the recruitment of co-repressors, such as histone-modifying enzymes including histone methyltransferases, histone deacetylases and lysine demethylases, to the promoter region of the target genes<sup>37,38</sup>. It is plausible that FREE1 might coordinate with other transcriptional repressors to function as a co-repressor in regulating ABA signalling, a scenario that is similar with the function mode of the DELLA transcriptional activator in gibberellin signalling<sup>39</sup> and the jasmonate ZIM-domain repressor in jasmonate signalling<sup>40</sup>. It will be interesting in the future to further identify the co-repressor proteins or the NINJA-like adaptors that work together with FREE1 to fine tune the activities of ABA-responsive transcription factors<sup>41</sup>.

Being a membrane-associated protein, FREE1 localizes to the endosomal (MVB) membrane through its FYVE domain via binding to PtdIns3P, a phosphoinositide predominantly enriched in the MVB in plant cells<sup>8</sup>. In addition, FREE1 is also detected in the soluble fraction<sup>8</sup> and shows a faint nuclear distribution pattern even without ABA treatment, as demonstrated in this study and another report<sup>13</sup>. Phosphatidylinositol 3-kinase and PtdIns3P have been detected in the plant nucleus<sup>42,43</sup>, which suggests that a small fraction of FREE1 might actively bind to nuclear-localized PtdIns3P to be involved in undefined nuclear phosphoinositide signalling events. Here, we found that ABA treatment lead to phosphorylation, and increased nuclear accumulation of FREE1 and nuclear FREE1 function as a transcriptional repressor. FREE1( $\Delta$ FYVE), which lost the binding ability to PtdIns3P, failed to recover the lethality of the *free1* loss-of-function mutant, suggesting that FREE1-mediated MVB biogenesis is essential for plant survival and the FYVE domain is key to FREE1-mediated MVB biogenesis. The largely genetic complementation of *free1-ctmut* by FREE1( $\Delta$ FYVE) indicated that the ABA hypersensitivity of *free1-ctmut* was less likely caused by a defect in MVB-mediated vacuolar sorting and degradation of ABA receptors. Our data indicate that FREE1 plays additional functions in the nucleus to transcriptionally modulate ABA signalling. For FREE1 functions in the regulation of ABA signalling, we are currently not able to distinguish which fraction of FREE1 functions, MVB related or nucleus related, play a more important role in ABA signalling, because the MVB-localized FREE1 is essential for plant growth and it is not able to obtain the transgenic plants such *free1*/FREE1( $\Delta$ FYVE) for ABA-responsive study owing to its seedling lethality. The dual-functional mode of FREE1, which either acts as an essential positive player in the ESCRT-dependent vacuolar trafficking pathway or functions as a nuclear transcriptional repressor for pulsed response to ABA to subsequently desensitize the cell to ABA responses, provokes the possibility that ABA responses at cellular level may include both transcriptional events in the nucleus as well as modulation of the FREE1-dependent vacuolar sorting pathway in the cytosol. Thus, it is highly possible that a sort of trade-off relationship exists between the FREE1-mediated vacuolar trafficking of certain vacuolar proteins and ABA-responsible molecules in specific abiotic stress conditions, although this notion still lacks evidence. One possibility is that ABA treatment or other abiotic stress, such as drought, might retard the MVB-mediated endosomal sorting route; thus, as feedback, the endosomal sorting regulator FREE1 might shuttle to the nucleus to attenuate ABA signalling and

to relieve ABA-mediated inhibition on endosomal sorting. Such a hypothesis is an interesting option to be further explored.

## Methods

**Plant materials.** The *Arabidopsis free1* mutant used in this study had been described previously<sup>8</sup>. The *Arabidopsis abf4*, *abi5-8* and *snrk2.2/2.3/2.6* had been described previously<sup>29,44,45</sup>. Seeds were surface sterilized and grown on plates with 1/2× MS (MSP01-50LT, Caisson Labs) plus 1% sucrose and 0.8% phyto agar at 22 °C under a long-day (16-h light/8-h dark) photoperiod.

### Detached leaf senescence and measurement of chlorophyll content.

The detached leaf senescence experiment was performed according to the methods described previously<sup>39</sup>. Rosette leaves from 4-week-old soil grown plants were detached and soaked in water with or without 50  $\mu$ M ABA. After 72 h of treatment, the leaves were moved to plates for photographing and measurement of chlorophyll content. Chlorophyll was extracted with (80% acetone) and quantified spectrophotometrically at 663 nm and 645 nm, respectively, followed by calculation using the previously established formula as  $(20.21 \times OD_{645} + 8.02 \times OD_{663}) / 1,000 \times V/W$ <sup>46</sup>, where 'V' indicates volume of extraction buffer (ml) and 'W' indicates fresh weight of leaves (g).

**Dual-luciferase reporter assay.** Protoplasts were isolated from the rosette leaves of 3-week-old Col-0. The *LUC* gene under the control of the 2,000-bp promoter sequences of *PAO1* or *EM6*, respectively, in the pGreenII 0800-LUC vector was generated as a reporter. The Renilla luciferase (*REN*) gene under the control of 35S promoter in the pGreenII 0800-LUC vector was used as the internal control, and 35Spro::GFP, 35Spro::GFP-FREE1, 35Spro::ABF4 and 35Spro::ABI5 constructs were used as effectors<sup>47</sup>. For ABA treatment, protoplasts were incubated with 50  $\mu$ M ABA overnight at room temperature after transformation. The firefly *LUC* and *REN* activities were quantified using a dual-luciferase assay kit (Promega). *LUC*/*REN* ratios were presented and the groups expressing 35Spro::GFP with 35S::ABF4 or 35Spro::ABI5 were arbitrarily set to 1. At least three transient assay measurements were contained for each assay.

**Co-immunoprecipitation analysis.** The co-immunoprecipitation assay was carried out according to our previously established method<sup>8</sup>. The samples of 0.5 g 6-day-old seedlings tissue were freeze grounded to powder and homogenized in 2 ml IP buffer (50 mM Tris-HCl, pH 7.4, 150 mM NaCl, 1 mM MgCl<sub>2</sub>, 20% glycerol, 0.2% NP-40, 1× protease inhibitor cocktail and 1× phosphatase inhibitor cocktail from Roche). Lysates were clarified by centrifugation at 14,000 r.p.m. for 15 min at 4 °C and were incubated with GFP-Trap agarose beads (ChromoTek) for 4 h at 4 °C in a top to end rotator. After incubation, the beads were washed five times with ice-cold washing buffer (50 mM Tris-HCl, pH 7.4, 150 mM NaCl, 1 mM MgCl<sub>2</sub>, 20% glycerol and 0.02% NP-40) and then eluted by boiling in reducing SDS sample buffer. Samples were separated by SDS-PAGE and analysed by immunoblot using appropriate antibodies. For mass spectrometry analysis, the gel was stained with silver or Coomassie blue after SDS-PAGE separation, and the interesting protein bands were cut out for in-gel trypsin digestion as described previously<sup>48</sup>, followed by mass spectrometry analysis at the Guangzhou Fitgene Biotechnology Company.

**Western blot analysis of phosphorylated proteins.** To analyse the phosphorylation of the GFP-tagged FREE1 protein, 6-day-old transgenic plants expressing the corresponding GFP fusions were freeze grounded to powder and homogenized in 1 ml IP buffer (50 mM Tris-HCl, pH 7.4, 150 mM NaCl, 20% glycerol, 0.2% NP-40, 1× protease inhibitor cocktail and 1× phosphatase inhibitor cocktail from Roche). Lysates were clarified by centrifugation at 14,000 r.p.m. for 15 min at 4 °C and were immunoprecipitated with GFP-Trap. After incubation, the beads were washed five times with ice-cold washing buffer (50 mM Tris-HCl, pH 7.4, 150 mM NaCl, 20% glycerol and 0.02% NP-40) and then eluted by boiling in reducing SDS sample buffer. Samples were separated by SDS-PAGE and transferred to a PVDF (polyvinylidene difluoride) membrane followed by probe with Phos-tag BTL-111 according to the manufacturer's instructions ([www.wako-chem.co.jp](http://www.wako-chem.co.jp)). In addition, to observe the total protein amount of immunoprecipitated GFP fusions used for Phos-tag detection, the same amount of immunoprecipitated proteins from each sample was also separated by SDS-PAGE followed by western blotting analysis with anti-GFP antibody. The chemiluminescence was imaged using an image analyser (ChemiDoc, Bio-Rad).

**In vitro phosphorylation assay of FREE1.** The in vitro phosphorylation assay was carried out essentially according to the methods described previously<sup>27</sup>. His-Sumo-FREE1, His-Sumo-FREE1(S530AS533A), His-Sumo-GFP, His-MBP-Snrk2.2 and His-MBP-Snrk2.3 fusion proteins were expressed and purified from *E. coli* (Rosetta) or *E. coli* (BL21) with Ni-NTA resin. YFP-tagged Snrk2.2 and Snrk2.3 proteins were obtained by immunoprecipitation from YFP-Snrk2.2 and YFP-Snrk2.3 transgenic plants treated with 100  $\mu$ M ABA for 30 min. Six-day-old plants treated with 0.5 g ABA were used for total protein extraction followed by immunoprecipitation with 10  $\mu$ l GFP-Trap. For in vitro kinase assays, immunoprecipitated YFP-Snrk2.2 and YFP-Snrk2.3 or purified His-MBP-

SnRK2.2 and His-MBP-SnRK2.3 were incubated with purified His-Sumo-FREE1, His-Sumo-FREE1(S530A/S533A) or His-Sumo-GFP in 30 µl kinase buffer (10 mM Tris-HCl, pH 7.8, 10 mM MgCl<sub>2</sub>, 0.5 mM dithiothreitol, 2 mM MnCl<sub>2</sub>, and 50 mM ATP) for 1 h at room temperature. Samples were separated by SDS-PAGE and transferred to a PVDF membrane followed by probe with Phos-tag BTL-111. In addition, to observe the total protein amount of His-Sumo fusions and SnRK2 proteins used for Phos-tag detection, the same amount of protein from each sample was also separated by SDS-PAGE followed by either Coomassie brilliant blue staining or western blotting analysis with anti-GFP antibody.

**ChIP assay.** The ChIP assay was performed following the procedures as described<sup>49</sup>. Six-day-old UBQ::YFP-ABF4/WT and UBQ::YFP-ABF4/*free1-ctmut* transgenic plants grown on 1/2× MS medium either lacking or supplemented with 0.5 µM ABA. The transgenic plants expressing GFP only were used as control for the ChIP assay. The chromatin was sheared to an average length of 500 bp by sonication-assisted extraction, followed by immunoprecipitation with GFP-Trap. Then, the DNA associated with the immunoprecipitated proteins was analysed by qRT-PCR. The level of binding was calculated as the ratio between immunoprecipitation and input.

**Data quantification and statistical analysis.** The relative intensities of each band detected with phos-tag and anti-GFP were quantified using ImageJ (<https://imagej.nih.gov/ij/>); the first lane in each experiment was set as 1. The relative fluorescence intensity of the nucleus and whole cells were quantified using ImageJ, and the ratios of fluorescence intensities (nucleus/whole cell in individual optical sections) are shown and the ratios of plants grown on 1/2× MS medium were arbitrarily set to 1. Data were analysed using SPSS version 13.0 statistical software (SPSS Inc.). Diagrams were prepared using Sigmaplot 11.0 (Systat Software Inc.). The data are presented as means ± standard errors (s.e.) and the circles in the bar graphs present in a format that shows data distribution (dot plots). Statistically significant differences were determined by one-way analysis of variance (ANOVA) followed by Tukey's multiple test as shown in each figure legend.

**Reporting Summary.** Further information on research design is available in the Nature Research Reporting Summary linked to this article.

## Data availability

The data that support the findings of this study are available from the corresponding authors on reasonable request.

Received: 26 September 2018; Accepted: 5 March 2019;

Published online: 08 April 2019

## References

- Henne, W. M., Buchkovich, N. J. & Emr, S. D. The ESCRT pathway. *Dev. Cell* **21**, 77–91 (2011).
- Liu, C., Shen, W., Yang, C., Zeng, L. & Gao, C. Knowns and unknowns of plasma membrane protein degradation in plants. *Plant Sci.* **272**, 55–61 (2018).
- Leung, K. F., Dacks, J. B. & Field, M. C. Evolution of the multivesicular body ESCRT machinery; retention across the eukaryotic lineage. *Traffic* **9**, 1698–1716 (2008).
- Valencia, J. P., Goodman, K. & Otegui, M. S. Endocytosis and endosomal trafficking in plants. *Annu. Rev. Plant Biol.* **67**, 309–335 (2016).
- Gao, C., Zhuang, X., Shen, J. & Jiang, L. Plant ESCRT complexes: moving beyond endosomal sorting. *Trends Plant Sci.* **22**, 986–998 (2017).
- Otegui, M. S. ESCRT-mediated sorting and intraluminal vesicle concatenation in plants. *Biochem. Soc. Trans.* **46**, 537–545 (2018).
- Buono, R. A. et al. ESCRT-mediated vesicle concatenation in plant endosomes. *J. Cell Biol.* **216**, 2167–2177 (2017).
- Gao, C. et al. A unique plant ESCRT component, FREE1, regulates multivesicular body protein sorting and plant growth. *Curr. Biol.* **24**, 2556–2563 (2014).
- Kolb, C. et al. FYVE1 is essential for vacuole biogenesis and intracellular trafficking in *Arabidopsis*. *Plant Physiol.* **167**, 1361–1373 (2015).
- Shen, J. B. et al. AtBRO1 functions in ESCRT-I complex to regulate multivesicular body protein sorting. *Mol. Plant* **9**, 760–763 (2016).
- Zhuang, X. et al. A BAR-domain protein SH3P2, which binds to phosphatidylinositol 3-phosphate and ATG8, regulates autophagosome formation in *Arabidopsis*. *Plant Cell* **25**, 4596–4615 (2013).
- Gao, C. et al. Dual roles of an *Arabidopsis* ESCRT component FREE1 in regulating vacuolar protein transport and autophagic degradation. *Proc. Natl Acad. Sci. USA* **112**, 1886–1891 (2015).
- Barberon, M. et al. Polarization of IRON-REGULATED TRANSPORTER 1 (IRT1) to the plant–soil interface plays crucial role in metal homeostasis. *Proc. Natl Acad. Sci. USA* **111**, 8293–8298 (2014).
- Miyakawa, T., Fujita, Y., Yamaguchi-Shinozaki, K. & Tanokura, M. Structure and function of abscisic acid receptors. *Trends Plant Sci.* **18**, 259–266 (2013).
- Yu, F. & Xie, Q. Non-26S proteasome endomembrane trafficking pathways in ABA signaling. *Trends Plant Sci.* **22**, 976–985 (2017).
- Yu, F., Wu, Y. R. & Xie, Q. Precise protein post-translational modifications modulate ABI5 activity. *Trends Plant Sci.* **20**, 569–575 (2015).
- Kong, L. et al. Degradation of the ABA co-receptor ABI1 by PUB12/13 U-box E3 ligases. *Nat. Commun.* **6**, 8630 (2015).
- Belda-Palazon, B. et al. FYVE1/FREE1 interacts with the PYL4 ABA receptor and mediates its delivery to the vacuolar degradation pathway. *Plant Cell* **28**, 2291–2311 (2016).
- Yu, F. F. et al. ESCRT-I component VPS23A affects ABA signaling by recognizing ABA receptors for endosomal degradation. *Mol. Plant* **9**, 1570–1582 (2016).
- Bueso, E. et al. The single-subunit RING-type E3 ubiquitin ligase RSL1 targets PYL4 and PYR1 ABA receptors in plasma membrane to modulate abscisic acid signaling. *Plant J.* **80**, 1057–1071 (2014).
- Rodríguez, L. et al. C2-domain abscisic acid-related proteins mediate the interaction of PYR/PYL/RCAR abscisic acid receptors with the plasma membrane and regulate abscisic acid sensitivity in *Arabidopsis*. *Plant Cell* **26**, 4802–4820 (2014).
- Zhao, Q. et al. Fast-suppressor screening for new components in protein trafficking, organelle biogenesis and silencing pathway in *Arabidopsis thaliana* using DEX-inducible FREE1-RNAi plants. *J. Genet. Genomics* **42**, 319–330 (2015).
- Shen, J. et al. A plant Bro1 domain protein BRAF regulates multivesicular body biogenesis and membrane protein homeostasis. *Nat. Commun.* **9**, 3784 (2018).
- Gao, X., Chen, J., Dai, X., Zhang, D. & Zhao, Y. An effective strategy for reliably isolating heritable and Cas9-free *Arabidopsis* mutants generated by CRISPR/Cas9-mediated genome editing. *Plant Physiol.* **171**, 1794–1800 (2016).
- Gao, Y. B. & Zhao, Y. D. Self-processing of ribozyme-flanked RNAs into guide RNAs in vitro and in vivo for CRISPR-mediated genome editing. *J. Integr. Plant Biol.* **56**, 343–349 (2014).
- Raghavendra, A. S., Gonugunta, V. K., Christmann, A. & Grill, E. ABA perception and signalling. *Trends Plant Sci.* **15**, 395–401 (2010).
- Planes, M. D. et al. A mechanism of growth inhibition by abscisic acid in germinating seeds of *Arabidopsis thaliana* based on inhibition of plasma membrane H<sup>+</sup>-ATPase and decreased cytosolic pH, K<sup>+</sup>, and anions. *J. Exp. Bot.* **66**, 813–825 (2015).
- Ng, L. M. et al. Structural basis for basal activity and autoactivation of abscisic acid (ABA) signaling SnRK2 kinases. *Proc. Natl Acad. Sci. USA* **108**, 21259–21264 (2011).
- Gao, S. et al. ABF2, ABF3, and ABF4 promote ABA-mediated chlorophyll degradation and leaf senescence by transcriptional activation of chlorophyll catabolic genes and senescence-associated genes in *Arabidopsis*. *Mol. Plant* **9**, 1272–1285 (2016).
- Nardozi, J. D., Lott, K. & Cingolani, G. Phosphorylation meets nuclear import: a review. *Cell Commun. Signal.* **8**, 32 (2010).
- Liu, Z. Y. et al. Plasma membrane CRPK1-mediated phosphorylation of 14-3-3 proteins induces their nuclear import to fine-tune CBF signaling during cold response. *Mol. Cell* **66**, 117–128 (2017).
- Nishino, T. G. et al. 14-3-3 regulates the nuclear import of class IIa histone deacetylases. *Biochem. Biophys. Res. Commun.* **377**, 852–856 (2008).
- Zhang, Z. et al. KETCH1 imports HYL1 to nucleus for miRNA biogenesis in *Arabidopsis*. *Proc. Natl Acad. Sci. USA* **114**, 4011–4016 (2017).
- Takeo, K. & Ito, T. Subcellular localization of VIP1 is regulated by phosphorylation and 14-3-3 proteins. *FEBS Lett.* **591**, 1972–1981 (2017).
- Yoshida, T. et al. Four *Arabidopsis* AREB/ABF transcription factors function predominantly in gene expression downstream of SnRK2 kinases in abscisic acid signalling in response to osmotic stress. *Plant Cell Environ.* **38**, 35–49 (2015).
- Skubacz, A., Daszkowska-Golec, A. & Szarejko, I. The role and regulation of ABI5 (ABA-Insensitive 5) in plant development, abiotic stress responses and phytohormone crosstalk. *Front. Plant Sci.* **7**, 1884 (2016).
- Kagale, S. & Rozwadowski, K. EAR motif-mediated transcriptional repression in plants: an underlying mechanism for epigenetic regulation of gene expression. *Epigenetics* **6**, 141–146 (2011).
- Reynolds, N., O'Shaughnessy, A. & Hendrich, B. Transcriptional repressors: multifaceted regulators of gene expression. *Development* **140**, 505–512 (2013).
- Yoshida, H. et al. DELLA protein functions as a transcriptional activator through the DNA binding of the INDETERMINATE DOMAIN family proteins. *Proc. Natl Acad. Sci. USA* **111**, 7861–7866 (2014).
- Pauwels, L. & Goossens, A. The JAZ proteins: a crucial interface in the jasmonate signaling cascade. *Plant Cell* **23**, 3089–3100 (2011).
- Pauwels, L. et al. NINJA connects the co-repressor TOPLESS to jasmonate signalling. *Nature* **464**, 788–791 (2010).
- Bunney, T. D. et al. Association of phosphatidylinositol 3-kinase with nuclear transcription sites in higher plants. *Plant Cell* **12**, 1679–1688 (2000).
- Drobak, B. K. & Heras, B. Nuclear phosphoinositides could bring FYVE alive. *Trends Plant Sci.* **7**, 132–138 (2002).

44. Zhou, X. N. et al. SOS2-LIKE PROTEIN KINASE5, an SNF1-RELATED PROTEIN KINASE3-type protein kinase, is important for abscisic acid responses in *Arabidopsis* through phosphorylation of ABSCISIC ACID-INSENSITIVE5. *Plant Physiol.* **168**, 659–676 (2015).
45. Nakashima, K. et al. Three *Arabidopsis* SnRK2 protein kinases, SRK2D/SnRK2.2, SRK2E/SnRK2.6/OST1 and SRK2I/SnRK2.3, involved in ABA signaling are essential for the control of seed development and dormancy. *Plant Cell Physiol.* **50**, 1345–1363 (2009).
46. Benedetti, C. E. & Arruda, P. Altering the expression of the chlorophyllase gene *ATHCOR1* in transgenic *Arabidopsis* caused changes in the chlorophyll-to-chlorophyllide ratio. *Plant Physiol.* **128**, 1255–1263 (2002).
47. Song, S. et al. Interaction between MYC2 and ETHYLENE INSENSITIVE3 modulates antagonism between jasmonate and ethylene signaling in *Arabidopsis*. *Plant Cell* **26**, 263–279 (2014).
48. Gao, C. et al. The Golgi-localized *Arabidopsis* endomembrane protein 12 contains both endoplasmic reticulum export and Golgi retention signals at its C terminus. *Plant Cell* **24**, 2086–2104 (2012).
49. Yamaguchi, N. et al. Protocols: chromatin immunoprecipitation from *Arabidopsis* tissues. *Arabidopsis Book* **12**, e0170 (2014).

## Acknowledgements

This work was supported by grants from the National Natural Science Foundation of China (31671467 and 31870171), the China 1000-Talents Plan for young researchers (C83025) to C.G., the National Natural Science Foundation of China (31701246) to W.S., the China Postdoctoral Science Foundation (2018M630963) and the National Science

Foundation of Guangdong Province (2018A030310505) to C.Y., the National Natural Science Foundation of China (91854201) and the Research Grants Council of Hong Kong (C4011-14R, C4012-16E, C4002-17G and AoE/M-05/12) to L.J. We thank H. Deng for her assistance on the EMSA experiments.

## Author contributions

H.L., Y.L., Q.Z. and C.G. designed the project. H.L., Y.L., Q.Z., T.L., J.W., B.L. and Y.Z. performed the experiments. H.L., Y.L., Q.Z., W.S., C.Y., P.L.R., Y.Z., L.J., X.W. and C.G. analysed the results. H.L., Q.Z., R.L.R., L.J., X.W. and C.G. wrote the manuscript.

## Competing interests

The authors declare no competing interests.

## Additional information

**Supplementary information** is available for this paper at <https://doi.org/10.1038/s41477-019-0400-5>.

**Reprints and permissions information** is available at [www.nature.com/reprints](http://www.nature.com/reprints).

**Correspondence and requests for materials** should be addressed to L.J., X.W. or C.G.

**Journal peer review information:** *Nature Plants* thanks Masa Sato and other anonymous reviewers for their contribution to the peer review of this work.

**Publisher's note:** Springer Nature remains neutral with regard to jurisdictional claims in published maps and institutional affiliations.

© The Author(s), under exclusive licence to Springer Nature Limited 2019

## Reporting Summary

Nature Research wishes to improve the reproducibility of the work that we publish. This form provides structure for consistency and transparency in reporting. For further information on Nature Research policies, see [Authors & Referees](#) and the [Editorial Policy Checklist](#).

### Statistics

For all statistical analyses, confirm that the following items are present in the figure legend, table legend, main text, or Methods section.

n/a Confirmed

- |                                     |                                     |  |
|-------------------------------------|-------------------------------------|--|
| <input type="checkbox"/>            | <input checked="" type="checkbox"/> | The exact sample size ( $n$ ) for each experimental group/condition, given as a discrete number and unit of measurement  |
| <input type="checkbox"/>            | <input checked="" type="checkbox"/> | A statement on whether measurements were taken from distinct samples or whether the same sample was measured repeatedly  |
| <input type="checkbox"/>            | <input checked="" type="checkbox"/> | The statistical test(s) used AND whether they are one- or two-sided<br><i>Only common tests should be described solely by name; describe more complex techniques in the Methods section.</i>   |
| <input checked="" type="checkbox"/> | <input type="checkbox"/>            | A description of all covariates tested   |
| <input checked="" type="checkbox"/> | <input type="checkbox"/>            | A description of any assumptions or corrections, such as tests of normality and adjustment for multiple comparisons  |
| <input type="checkbox"/>            | <input checked="" type="checkbox"/> | A full description of the statistical parameters including central tendency (e.g. means) or other basic estimates (e.g. regression coefficient) AND variation (e.g. standard deviation) or associated estimates of uncertainty (e.g. confidence intervals) |
| <input type="checkbox"/>            | <input checked="" type="checkbox"/> | For null hypothesis testing, the test statistic (e.g. $F$ , $t$ , $r$ ) with confidence intervals, effect sizes, degrees of freedom and $P$ value noted<br><i>Give <math>P</math> values as exact values whenever suitable.</i>                            |
| <input checked="" type="checkbox"/> | <input type="checkbox"/>            | For Bayesian analysis, information on the choice of priors and Markov chain Monte Carlo settings   |
| <input checked="" type="checkbox"/> | <input type="checkbox"/>            | For hierarchical and complex designs, identification of the appropriate level for tests and full reporting of outcomes   |
| <input type="checkbox"/>            | <input checked="" type="checkbox"/> | Estimates of effect sizes (e.g. Cohen's $d$ , Pearson's $r$ ), indicating how they were calculated   |

*Our web collection on [statistics for biologists](#) contains articles on many of the points above.*

### Software and code

Policy information about [availability of computer code](#)

- |                 |   |
|-----------------|---|
| Data collection | <input type="text" value="Bio-Rad ChemiDoc Touch Imaging Software V1.2, ZEISS ZEN software V.2011, Bio-Rad CFX Maestro Software"/>                                    |
| Data analysis   | <input type="text" value="SPSS version 13.0 statistical software (SPSS Inc., Chicago, USA), Sigmaplot version 11.0 (Systat Software Inc., San Jose, USA), Image J."/> |

For manuscripts utilizing custom algorithms or software that are central to the research but not yet described in published literature, software must be made available to editors/reviewers. We strongly encourage code deposition in a community repository (e.g. GitHub). See the Nature Research [guidelines for submitting code & software](#) for further information.

### Data

Policy information about [availability of data](#)

All manuscripts must include a [data availability statement](#). This statement should provide the following information, where applicable:

- Accession codes, unique identifiers, or web links for publicly available datasets
- A list of figures that have associated raw data
- A description of any restrictions on data availability

## Field-specific reporting

Please select the one below that is the best fit for your research. If you are not sure, read the appropriate sections before making your selection.

- Life sciences       Behavioural & social sciences       Ecological, evolutionary & environmental sciences

For a reference copy of the document with all sections, see [nature.com/documents/nr-reporting-summary-flat.pdf](http://nature.com/documents/nr-reporting-summary-flat.pdf)

# Life sciences study design

All studies must disclose on these points even when the disclosure is negative.

Sample size	No statistical method was used to predetermine the sample sizes. Sample sizes were chosen as large as possible while still practically doable in terms of data collection and as sufficient when results could be reliably reproduced. For Co-IP, CHIP, Western blotting, protein phosphorylation assay, qPCR analyses, three biological replicates were performed. Each replicate contained a group of Arabidopsis seedlings weighing about 0.5 g to 2 g. For chlorophyll contents analyses, three biological replicates were used. Each biological replicate contained 20 randomly picked leaves. For confocal observation of GFP-FREE1 localization, three biological replicates were used. 10 individual seedlings were observed for each biological replicate. For seedling establishment analysis in response to ABA treatment, three biological replicates were performed. Around 150 seeds of each genotype were used for seedling establishment analysis in each biological replicates. For BiFC and dual-LUC assay, three biological replicates were used. Around 40000 protoplasts were used for each plasmid transfection in each biological replicate. For TEM study, 15 Arabidopsis root tips of each genotype were randomly selected for high pressure freezing. A minimum of three blocks (each block contains 1-2 root tips) from each sample were randomly selected for sectioning and TEM imaging.
Data exclusions	No data were excluded from the analysis.
Replication	For the mass spectrometry experiment shown in Supplementary 11 and ABA-induced phosphorylation of FREE1 as shown in Supplementary Figure 9, two times experiments were performed with similar outcomes obtained. The other major experimental findings were reliably reproduced at least three times in this study.
Randomization	The Arabidopsis seedlings with the same genetic background were randomly placed in the culture medium with/without abscisic acid treatments. The Arabidopsis seedlings or protoplasts were randomly selected for confocal observation. The yeast colonies in SD-2 medium were randomly picked for growth assay in the more stringent SD-3 or SD-4 medium.
Blinding	The investigators were blinded to group allocation during data collection and analysis.

## Reporting for specific materials, systems and methods

We require information from authors about some types of materials, experimental systems and methods used in many studies. Here, indicate whether each material, system or method listed is relevant to your study. If you are not sure if a list item applies to your research, read the appropriate section before selecting a response.

### Materials & experimental systems

n/a	Involvement in the study
<input type="checkbox"/>	<input checked="" type="checkbox"/> Antibodies
<input checked="" type="checkbox"/>	<input type="checkbox"/> Eukaryotic cell lines
<input checked="" type="checkbox"/>	<input type="checkbox"/> Palaeontology
<input checked="" type="checkbox"/>	<input type="checkbox"/> Animals and other organisms
<input checked="" type="checkbox"/>	<input type="checkbox"/> Human research participants
<input checked="" type="checkbox"/>	<input type="checkbox"/> Clinical data

### Methods

n/a	Involvement in the study
<input checked="" type="checkbox"/>	<input type="checkbox"/> ChIP-seq
<input checked="" type="checkbox"/>	<input type="checkbox"/> Flow cytometry
<input checked="" type="checkbox"/>	<input type="checkbox"/> MRI-based neuroimaging

## Antibodies

Antibodies used	FREE1 antibody (Gao et al., Current Biology, 2014, 24, 2556-2563) was homemade as described in our previous publication. Other antibodies used in this study are commercially available (Histone H3 antibody, Abcam, Cat. No. ab1791; FBpase antibody, Agrisera, Cat. No. AS04043; H <sup>+</sup> -ATPase antibody, Agrisera, Cat. No. AS07260; GFP antibody, Abcam, Cat. No. ab290).
Validation	FREE1 antibody (Gao et al., Current Biology, 2014, 24, 2556-2563) was homemade as described and validated in our previous publication. Validation statement for Histone H3 antibody (Abcam, Cat. No. ab1791) can be found at the product website.< <a href="https://www.abcam.com/histone-h3-antibody-nuclear-loading-control-and-chip-grade-ab1791.html">https://www.abcam.com/histone-h3-antibody-nuclear-loading-control-and-chip-grade-ab1791.html</a> > Validation statement for FBpase antibody (Agrisera, Cat. No. AS04043) can be found at the product website.< <a href="https://www.agrisera.com/en/artiklar/cfbpase-cytosolic-fructose-16-bisphosphatase-marker-for-cytoplasm.html">https://www.agrisera.com/en/artiklar/cfbpase-cytosolic-fructose-16-bisphosphatase-marker-for-cytoplasm.html</a> > Validation statement for H <sup>+</sup> -ATPase antibody(Agrisera, Cat. No. AS07260) can be found at the product website.< <a href="https://www.agrisera.com/en/artiklar/hatpase-plasma-membrane-hatpase.html">https://www.agrisera.com/en/artiklar/hatpase-plasma-membrane-hatpase.html</a> > Validation statement for GFP antibody (Abcam, Cat. No. ab290) can be found at the product website.< <a href="https://www.abcam.com/gfp-antibody-chip-grade-ab290.html">https://www.abcam.com/gfp-antibody-chip-grade-ab290.html</a> >